Article:
Colley, HE, Hearnden, V, Avila-Olias, M et al. (2014) Polymersome-Mediated Delivery of Combination Anticancer Therapy to Head and Neck Cancer Cells: 2D and 3D in Vitro Evaluation. Molecular Pharmaceutics, 11 (4). pp. 1176-1188. ISSN: 1543-8384

https://doi.org/10.1021/mp400610b

Polymersome-mediated delivery of combination anti-cancer therapy to head and neck cancer cells: 2D and 3D *in vitro* evaluation

Helen E. Colley[1,2,#], Vanessa Hearnden[1,2,3 #], Milagros Avila-Olias[2,4,5, #], Denis Cecchin[2,5,6], Irene Canton[2], Jeppe Madsen[2,7], Sheila MacNeil[3], Nicholas Warren[2,7], Ke Hu[8], Jane A McKeating[8], Steven P. Armes[7], Craig Murdoch[1,], Martin H. Thornhill[1] and Giuseppe Battaglia[2,5,6,*]

[1] School of Clinical Dentistry, University of Sheffield, Sheffield, UK

[2] Department of Biomedical Science, University of Sheffield, Sheffield, UK

[3] Department of Materials Science and Engineering, Sheffield, UK

[4]The Centre for Membrane Interactions and Dynamics, University of Sheffield, Sheffield, UK

[5] Department of Chemistry, University College London, London, UK

[6]The MRC/UCL Centre for Medical Molecular Virology, University College London, London, UK

[7]Department of Chemistry, University of Sheffield, Sheffield, UK

[8] Institute for Biomedical Research, University of Birmingham, Birmingham, UK.

*Corresponding authors:

Professor Giuseppe Battaglia, Department of Chemistry and The MRC/UCL Centre for Medical Molecular Virology, University College London , 20 Gordon Street, London WC1H 0AJ, UK.

Email: g.battaglia@ucl.ac.uk

[#]These authors contributed equally to this study.

Abstract

Polymersomes have the potential to encapsulate and deliver chemotherapeutic drugs into tumour cells, reducing off-target toxicity that often compromises anti-cancer treatment. Here we assess the ability of the pH-sensitive poly 2-(methacryloyloxy)ethyl phosphorylcholine (PMPC)- poly 2-(diisopropylamino)ethyl methacrylate (PDPA) polymersomes to encapsulate chemotherapeutic agents for effective combinational anti-cancer therapy. Polymersome uptake and ability to deliver encapsulated drugs into healthy normal oral cells and oral head and neck squamous cell carcinoma (HNSCC) cells was measured in two and three-dimensional culture systems. PMPC-PDPA polymersomes were more rapidly internalised by HNSCC cells compared to normal oral cells. Polymersome cellular up-take was found to be mediated by class B scavenger receptors. We also observed that these receptors are more highly expressed by cancer cells compared to normal oral cells, enabling polymersome-mediated targeting. Doxorubicin and paclitaxel were encapsulated into pH-sensitive PMPC-PDPA polymersomes with high efficiencies either in isolation or as a dual-load for both singular and combinational delivery. In monolayer culture, only a short exposure to drug-loaded polymersomes was required to elicit a strong cytotoxic effect. When delivered to three-dimensional tumour models, PMPC-PDPA polymersomes were able to penetrate deep into the centre of the spheroid resulting in extensive cell damage when loaded with both singular and dual-loaded chemotherapeutics. PMPC-PDPA polymersomes offer a novel system for the effective delivery of chemotherapeutics for the treatment of HNSCC. Moreover, the preferential internalisation of PMPC polymersomes by exploiting elevated scavenger receptor expression on cancer cells opens up the opportunity to target polymersomes to tumours.

Keywords: Polymersomes, drug delivery, paclitaxel, doxorubicin, head and neck cancer, multi-cellular tumour spheroid, scavenger receptors.

Introduction

Appropriate and effective delivery is vital to a drug's therapeutic success. In order for a drug to exert its therapeutic effect it must be delivered to the target cells, at the optimum dose and in its active form. Drugs delivered inappropriately to healthy tissues and organs can produce off-target effects that may limit the dose that these drugs can be administered, resulting in sub-optimal or even abandoned treatment. Many anti-cancer drugs target cell proliferation by utilising the abnormal growth of cancerous cells. For example, doxorubicin acts by intercalating the DNA to inhibit cell division. Unfortunately, doxorubicin administration is associated with severe cardiotoxicity, limiting its use[1]. Poor drug solubility is also a great challenge in drug development. The commonly used anti-cancer agent paclitaxel is a potent inhibitor of mitosis but is poorly soluble in water (aqueous solubility is around 0.6 mM)[2]. Paclitaxel is therefore administered in conjunction with the stabilizing agent Kolliphor EL (formally known as Cremophor EL) to ensure that therapeutically sufficient doses are delivered to the patient. However, Kolliphor EL has been associated with acute hypersensitivity reactions and systemic immunostimulation in some patients that limits its use[3]. Long systemic circulation times and reduced clearance by the reticular endothelium system are also crucial if drugs are to be delivered to tissues at therapeutic concentrations.

The last decade has seen a dramatic increase in research into the use of various nanoparticles to deliver therapeutic agents to overcome some of these challenges. Since the pioneering work of Maeda and co-workers[4], it is now well established that the leaky vasculature associated with tumour growth favours the accumulation of macromolecules and nanocarriers in the tumour due the enhanced permeability and retention (EPR) effect[4]. This observation has lead to the development of several nanoparticles that act as carriers and passively target solid tumours.

Several of these have now reached the clinic including Doxil® (Caelyx®), a polyethylene glycol (PEG)-conjugated liposome formulation of doxorubicin that shows reduced cardiotoxicity compared to doxorubicin alone[5]. However, Doxil® therapy is not without its own side-effects as its use has resulted in hand-foot syndrome in some patients[6]. These adverse effects are mitigated by using non-PEGylated liposomal formulations such as Myocet®[7]. However, these agents have much shorter circulation half-life in the blood and consequently less accumulation in tumours. A number of liposomal formulations for paclitaxel drug delivery are currently in clinical trials[8]. One of the main limitations of liposomal preparations is their short half-life and their inherent slow release of their therapeutic cargo which has led us and others to develop other synthetic alternatives[9,10]. Synthetic polymers are showing great promise[11] particularly in recent years where liposome and polymer technology have merged in the design of self-assembling membrane-enclosed structures comprised of block copolymers called polymersomes[12,13,14]. Polymersomes have been shown to exhibit longer half-lives and better tumour accumulation compared to PEGylated liposomes[15]. Advances in polymer synthesis techniques have enabled polymers to be designed with optimum properties for drug delivery including high molecular weights, enhanced stability, side chain functionality and more importantly, responsiveness [12-14, 16].

Cancers originating in the head and neck region and oral cavity are potentially more accessible to local chemotherapeutic drug delivery[17] and could ultimately utilise the transmucosal delivery capability of these polymersomes seen *in vitro*[18]. Here we investigate the use of polymersomes comprised of the amphiphilic block copolymer poly 2-(methacryloyloxy)ethyl phosphorylcholine (PMPC) coupled with the pH-sensitive copolymer poly 2-(diisopropylamino)ethyl methacrylate (PDPA) for anti-cancer drug delivery. PMPC-PDPA polymersomes have been demonstrated to

be internalised via endocytosis[19] and dissociate within the low pH in the endosomal compartment, releasing their cargo into the cell cytosol[20]. Indeed, polymersomes have been used to deliver DNA, siRNA, proteins and antibodies into live cells[21, 22, 23, 24.]

The membrane-enclosed vesicular structure of polymersomes enables both hydrophilic and hydrophobic materials to be encapsulated within their aqueous core and the hydrophobic membrane respectively[25]. This is particularly important as combination therapies have been shown to improve response rates in head and neck squamous cell cancer (HNSCC)[26]. In this study, the internalization kinetics of PMPC-PDPA polymersomes into human HNSCC, normal oral cells and three-dimensional (3D) multi-cellular tumour spheroids (MCTS) were investigated. The ability of polymersomes to encapsulate chemotherapeutic drugs (paclitaxel and doxorubicin) and the effect of polymersome-mediated drug delivery were assessed both alone and in combination. Finally, uptake mechanisms were investigated to identify the target receptors involved in internalisation of polymersomes into cells.

Materials and Methods

All reagents were purchased from Sigma-Aldrich (Poole, UK) unless stated otherwise and used as described by the manufacturer's instructions.

$PMPC_{25}$-$PDPA_{70}$ copolymer synthesis

$PMPC_{25}$-$PDPA_{70}$ copolymer was synthesized by atom transfer radical polymerization (ATRP) as reported elsewhere[27]. Briefly, a Schlenk flask was charged with CuBr (25.6 mg, 0.178 mmol) and 2-Methacryloyloxyethyl phosphorylcholine (MPC) (1.32 g, 4.46 mmol; Biocompatibles Ltd). 2-bromo-2-methylpropanoate (ME-Br) initiator (50.0 mg, 0.178 mmol, prepared as in ([25])) and 2,2'-bipyridine ligand (bpy) (55.8 mg, 0.358 mmol) were dissolved in 2 ml methanol and the solution deoxygenated with N_2 for 30 minutes before being injected into the flask. The [MPC]:[ME-Br]:[CuBr]:[bpy] relative molar ratios were 25:1:1:2 respectively. The polymerization was conducted under a N_2 atmosphere at 20°C. After 65 minutes a mixture of deoxygenated 2-(Diisopropylamino)ethyl methacrylate (DPA) (2.67 g, 12.5 mmol; Scientific Polymer Products, USA) and methanol (3 ml) was injected into the flask, and after a further 48 h the reaction solution was diluted by adding 200 ml isopropanol and then passed through a silica column (Merk, Darmstadt, Germany) to remove spent Cu catalyst.

Rhodamine (Rho)-$PMPC_{30}PDPA_{60}$ copolymer synthesis

Rho-$PMPC_{30}$-$PDPA_{60}$ copolymer was synthesized by an ATRP procedure as previously described[27]. Briefly, a Schlenk flask was charged with MPC (1.20 g, 4.05 mmol). A rhodamine 6G-based initiator prepared in-house (83.8 mg, 0.135 mmol) was dissolved in methanol (0.75 ml) and added to the MPC. The solution was deoxygenated by bubbling N_2 for 30 minutes after

which a mixture of CuBr (19.37 mg, 0.135 mmol) and bpy ligand (42.17 mg, 0.171 mmol) was added to the reaction mixture. The [MPC]:[Rho]:[CuBr]:[bpy] relative molar ratios were 30:1:1:2 and the reaction was carried out under a N_2 atmosphere at 20°C. After 40 min, a mixture of deoxygenated DPA (1.73 g, 8.10 mmol) and methanol (2 ml) was injected into the flask and 48 h later the reaction solution was diluted with methanol (~70 ml) and opened to the atmosphere. When the suspension turned green, 200 ml chloroform was added to dissolve the copolymer and the solution passed through a silica column to remove the catalyst. After removal of the solvent, the solid was taken up into 3:1 chloroform:methanol and dialysed for 3 days against this solvent mixture to remove residual bpy ligand. After evaporation, the solid was dispersed in water, freeze-dried and dried in a vacuum oven at 80°C for 48 h.

Preparation and characterisation of chemotherapeutic loaded polymersomes

To produce polymersomes, 20 mg $PMPC_{25}$-$PDPA_{70}$ copolymer were dissolved in a 2:1 chloroform:methanol solution and a co-polymer film formed by evaporating the solvent overnight in a vacuum oven at 50°C. The film was rehydrated using 2 ml of 100 mM PBS for 7 days under continuous stirring. This solution was sonicated for 15 minutes and then purified by gel permeation chromatography using a sepharose 4B size exclusion column to extract the fraction containing vesicles (~200 nm in diameter by dynamic light scattering analysis) and remove any remaining impurities. To generate rhodamine-labelled polymersomes rho-$PMPC_{30}PDPA_{60}$ (5% v/v) was added to the $PMPC_{25}$-$PDPA_{70}$ prior to co-polymer film formation. To produce paclitaxel loaded polymersomes, 2 parts chloroform was mixed with 1 part methanol containing 500 µg paclitaxel prior to co-polymer film formation as described previously. The film was then rehydrated in 2 ml 100 mM PBS for 7 days under continuous stirring to produce

paclitaxel loaded polymersomes (250 µg/ml paclitaxel before purification; Table 1). Doxorubicin was encapsulated via a rehydration method as previously described[28]. Briefly, at the point of rehydration doxorubicin (final concentration 250 µg/ml) was added to the co-polymer film (either alone or paclitaxel loaded) in 2 ml of 100 mM PBS. The solution was then left for 7 days under continuous stirring at room temperature before sonication (15 min) and purification via gel permeation chromatography. Polymersome size was determined by dynamic light scattering and encapsulated drug concentrations determined by high performance liquid chromatography (Table 1).

Cell culture

This study used the following HNSCC cell lines: Cal27 (ATCC, Manassas, VA, USA), CRL-2095), FaDu (LGC Promochem, Middlesex, UK) and SCC4 (ECACC, Health Protection Agency Culture Collections, Salisbury, UK). Cal27 cells were cultured in Dulbecco's modified Eagle's medium (DMEM), FaDu in RPMI-1640 both supplemented with 10% (v/v) fetal calf serum (FCS; BioSera, East Sussex, UK), 2 mM L-Glutamine, 100 IU/ml penicillin and 100 mg/ml streptomycin and SCC4 in DMEM and Ham's F12 medium in a 1:1 (v/v) ratio supplemented with 10% (v/v) FCS, 2mM L-Glutamine, 100 IU/ml penicillin, 100 mg/ml streptomycin and 5 mg/ml hydrocortisone.

Normal oral keratinocytes (NOK) and fibroblasts (NOF) were isolated from biopsies obtained from the buccal and gingival oral mucosa from patients during routine dental procedures with written, informed consent (ethical approval number 09/H1308/66) as previously described[29]. Human dermal fibroblasts (HDF) were isolated from split thickness skin grafts obtained during

routine plastic surgery breast reduction and abdominoplasty operations, from fully consenting adults as previously described[30]. NOK were cultured in flavin and adenine enriched medium: DMEM and Ham's F12 medium in a 3:1 (v/v) ratio supplemented with 10% (v/v) FCS, 0.1 mM cholera toxin, 10 ng/ml of epidermal growth factor (EGF), 0.4 mg/ml hydrocortisone, 0.18mM adenine, 5 mg/ml insulin, 5 mg/ml transferrin, 2 mM glutamine, 0.2 mM triiodothyronine, 0.625 mg/ml amphotericin B, 100 IU/ml penicillin and 100 mg/ml streptomycin[31]. NOF and HDF were cultured in DMEM supplemented with 10% FCS, 2 mM glutamine, 100 IU ml penicillin and 100 mg/ml streptomycin. All cells were incubated at 37°C in 5% CO_2 and sub-cultured after brief treatment with trypsin-EDTA.

Multicellular spheroid formation

MCTS were generated from FaDu cells using the liquid overlay method as previously described[29]. Briefly, 100 ml of FaDu cells ($12x10^4$ per ml) were added to each well of a 96-well plate previously coated with 1.5% type V agarose (w/v in RPMI) and cultured for 4 days before being used for experiments.

Internalization kinetic analysis using flow cytometry

FaDu monolayers ($3x10^5$ per well) or MCTS were incubated with 300 µl or 100 µl of rho-labelled PMPC-PDPA polymersomes diluted in medium (1 mg/ml), respectively, and incubated at 37°C for increasing lengths of time. At each time point the media was removed and the cells washed 3 times with PBS, trypsinised and resuspended in 4% paraformaldehyde. Fixed cells were analysed using a FACSArray analyser (BD Biosciences) (excitation 532 nm, emission 564-606 nm) and the percentage of cells with fluorescence above control cells (cultured in media

alone) and median fluorescence of whole cell population calculated. Expression of scavenger receptors was assessed by flow cytometry in viable FaDu and HDF. Cells were incubated with primary antibody targeting either SR-BI or CD36 scavenger receptors (10 μg/ml) for 30 min at 4°C and then incubated with a fluorescently-labelled secondary antibody under the same conditions. Fluorescent microscope images of cell monolayers were captured using an Axon ImageXpress (Union City, CA) (excitation 560 nm and emission 607 nm). MCTS were frozen, sectioned, stained with DAPI and images captured using a Zeiss Axioplan 2 fluorescent microscope (Carl Zeiss Inc. Germany) with a Q-imaging Retiga 1300R camera (QI Imaging, Arizona, USA) and Image Pro Plus image software (Media Cybernetics, Inc., MD, USA).

Evaluation of cytotoxicity

Polymersomes loaded with paclitaxel, doxorubicin or dual loaded were incubated with FaDu monolayers or MCTS at increasing polymer concentrations (10, 50 and 100 μg/ml) and free drug equivalents. For short exposure experiments drug concentrations of 1 μg/ml were used for all groups. Cell metabolic activity was determined by 3-(4,5-dimethylthiazol-2-yl)-2,5-diphenyltetrazolium bromide (MTT) analysis. Briefly, cell monolayers or MCTS were incubated at 37°C for 1 h with 0.5 mg/ml MTT solution. Incorporated stain was eluted using 400 μl of acidified isopropanol and 100 μl transferred into a 96-well plate and the optical density measured spectrophotometrically at 570 nm, with a 630 nm correction reference. For MCTS, bright field images were captured at 24 and 96 h using a Zeiss Axiovert 200M light microscope (Carl Zeiss Inc., Germany), AxioCam MRm camera (Carl Zeiss Inc. Germany) and Axiovision Rel. 4.6 software (Carl Zeiss Inc., Germany).

Polymersome uptake blocking studies

FaDu, NOF or HDF ($5x10^5$) were seeded into a 24 well plates and allowed to attach overnight before incubation with fucoidan (0.5, 1 or 2 mg/ml) or polyinosinic acid (0.25, 0.1 or 0.05 mg/ml) for 30 minutes. For antibody blocking, cells were incubated with either anti-SR-BI/II (abcam), anti-CD36 (abcam) or IgG (abcam) all at a final concentration of 40 µg/mL for 1 h. For dual blocking cells were incubated with 20 µg/ml of both anti-SR-B1 and anti-CD 36 for 1 h. Cells were washed and incubated with rho-labelled polymersomes (1 mg/ml) for 1 h before being washed 3 times in PBS, trypsinised and fixed with 4% paraformaldehyde. Analysis was performed using a FACSArray analyser (BD Biosciences) (excitation 532 nm, emission 564-606 nm) and the percentage of cells with fluorescence above control cells (cultured in media alone) and median fluorescence of whole cell population calculated.

Immunoblotting

Cell pellets were washed twice with PBS and protein extracted using lysis buffer (Merck Millipore) containing Complete Mini Protease Inhibitor Cocktail (Roche; used according to manufacturer's instructions) and Benzonase (used according to manufacturer's instructions). Protein concentration was measured using BCA Protein Assay kit (ThermoScientific). Total protein extracts (40 µg) were separated by NuPAGE® 4-12% Bis-Tris Gels (Life Technologies) and transferred to nitrocellulose membrane using an iBlot gel transfer device (Life Technologies). Following blocking of non-specific protein binding in 5% (w/v) dried milk, 3% (w/v) BSA in Tris-buffered saline containing 0.5% (v/v) Tween 20, membranes were incubated with antibodies directed to anti-SR-BI (1:500, abcam) or anti-MSR (1:1000, abcam) and overnight at 4°C or β-actin (1:4000; Sigma-Aldrich) for 1 h at room temperature followed by

anti-mouse or anti-rabbit IgG horseradish peroxidase secondary antibody (1:2,000; Cell Signaling Technologies). All antibodies were diluted in 5% (w/v) dried milk, 3% (w/v) BSA in Tris-buffered saline containing 0.5% (v/v) Tween 20. Immunoreactive proteins were visualised using Pierce enhanced chemiluminescence (Thermo Scientific). Densitometry was performed using Quality One software (Bio-Rad).

Statistical analysis

Data are expressed as mean ± standard deviation and significant differences between groups examined using either the Student's unpaired *t*-test or one way independent ANOVA, with differences considered significant if $p<0.05$. Differences were mainly compared between HNSCC and NOK cells as NOK cells are epithelial and the most biologically comparable to HNSCC cell lines.

Results and Discussion

Cellular internalisation kinetics.

The site of action for most drugs lies within the cell, meaning intracellular delivery is crucial for therapeutic effect. Previous studies have shown that polymersomes are rapidly internalised by several cancer cell types where they enter endosomes[22], and so we aimed to determine if the internalisation rates of polymersomes into HNSCC cell lines was different to normal cells. Flow cytometric analysis showed that rhodamine-conjugated PMPC-PDPA polymersomes were internalised by all cell types examined but with considerably different kinetics depending on the cell type (Figure 1A). FaDu cells internalised the polymersomes very rapidly, with 70% of FaDu cells containing detectable levels of polymersomes after just 2 minutes exposure. Other HNSCC cell lines, Cal27 and SCC4, also showed rapid uptake with at least 70% of the population containing polymersomes after 10 minutes exposure. Compared to the HNSCC cell lines, the normal oral cells showed significantly slower (p<0.05) internalisation rates at all time points between 5 and 60 minutes. The rates of internalisation were similar after 180 minutes incubation. Normal oral keratinocytes (NOK) internalised polymersomes slightly faster than normal oral fibroblasts (NOF) and human dermal fibroblasts (HDF) but by 60 minutes approximately 70% of all three of the normal cell populations contained polymersomes. All the cell types tested showed over 90% of cells contained polymersomes after 180 minutes.

Faster internalisation into cancer cells compared to healthy cells is a highly desirable property when designing anti-cancer delivery systems as this may reduce adverse off-target effects. Our internalisation data indicates that polymersomes may be preferentially targeting cancer cells over normal cells.

In addition to the rate of uptake, it is also important to determine the relative amount of polymersomes being delivered to each cell type over time to give a clue as to the possible doses achievable using polymersome drug delivery. To analyse drug delivery the amount of rhodamine-conjugated polymersomes taken up by each cell type over time was measured and compared to their equivalent unexposed control cells. For all cell types tested the fluorescence intensity increased over time and continued to increase for up to 24 hours (Figure 1B). At all-time points examined between 5 and 480 minutes all three HNSCC cell lines contained significantly more polymersomes (p<0.01) when compared to the normal cells. The cells that internalised the most polymersomes per cell were the FaDu with the least polymersomes taken up by NOF (Figure 1B). Representative images of rhodamine-conjugated polymersomes internalised by FaDu cells demonstrate the increase in intensity over time (Figure 1C). These data show that HNSCC cells take up and accumulate polymersomes more rapidly than normal oral cells. The polymersomes tested here have an inherent ability to dissociate once they reach the low pH of the endosomal compartment, enabling fast release of their cargo into the cytosol after internalisation (Figure S1)[19]. This is in comparison to other delivery systems which exhibit good properties in the circulation but have difficulty releasing the cargo once internalised into target cells[32].

Class B Scavenger receptors mediate polymersome uptake in HNSCC cells and oral fibroblasts. To explain the increased uptake of polymersomes in cancer cells compared to normal cells we investigated the uptake mechanism. Previous studies in our laboratory have demonstrated that polymersomes are internalised via receptor-mediated endocytosis but the specific receptor/receptors have yet to be elucidated[19]. Recently, other groups have reported an

association between nanoparticle uptake and scavenger receptor expression[33], and recently a connection has been made between the differential expression of scavenger receptor type BI (SR-BI) between normal and cancerous cells[34]. Immunoblotting and densitometry were used to confirm the presence and relative expression of scavenger receptors in the different cell types and to determine if a different expression pattern was observed between normal oral and HNSCC cells. Expression of cell surface SR-BI (also known as CLA-1 (CD36 and LIMPII Analogous 1)) was higher in the HNSCC cell lines compared to the three normal cell types studied (Figure 2A-B). In addition, NOF had significantly lower expression of SR-BI compared to NOK. Expression of the class A receptor, MSR-1, was not observed in either normal or cancerous cells (data not shown).

The differences in the role of type B scavenger receptors in PMPC-PDPA binding and uptake between FaDu and fibroblasts could be a consequence of different expression patterns of these receptors on both cell types. In order to investigate this possibility we studied in detail, the cell surface expression of the type B receptors SR-BI and CD36 by FaDu and normal HDF cells using flow cytometry. Results in Figure 2C show the marked difference in scavenger receptor type B expression between these two cell types. FaDu cells express abundant cell surface SR-BI but only low levels of CD36, whereas HDF expressed low levels of SR-BI but high levels of CD36 (Figure 2C). Moreover, almost 100% of FaDu cells expressed SR-BI whilst the value for HDF was just 16%. In contrast, approximately 40% of FaDu cells expressed detectable levels of CD36 compared to almost 100% by HDF (Figure 2D). Therefore, FaDu cells express substantially more cell surface SR-BI than HDF. These results could explain the reason for the rapid internalisation of polymersomes by HNSCC cells compared to primary epithelial cells and fibroblasts.

Scavenger receptors control the uptake of high and low density lipoproteins, extracellular RNA and DNA, and mediate the internalisation of hepatitis C virus[35,35b]. Uptake of nanoparticles by scavenger receptors has recently been shown by Saha *et al* (2012), where gold-coated nanoparticle uptake was inhibited using polyinosinic acid, a specific inhibitor of class A scavenger receptors[33b]. In addition, Patel *et al* (2010) showed that scavenger receptor types A and B specifically mediated uptake of oligonucleotide-coated gold nanoparticles by HeLa cells [36]. More importantly, the phosphorylcholine groups expressed by the PMPC chains bode well for high affinity interaction with class B receptors as both CD36 and SR-BI are involved in the uptake of phosphorylcholine bearing phospholipids[16]. To study the role of SR-BI and CD36 in the uptake of PMPC-PDPA polymersomes we pre-incubated FaDu and NOF with Fucoidan and polyinosinic acid (well-known ligands for scavenger receptors). Fucoidan is an anionic polysaccharide that targets both class A and B scavenger receptors while polyinosinic acid, a single stranded polynucleotide of inosine, specifically targets scavenger receptor type A[37]. Following pre-incubation with these ligands, cells were incubated with polymersomes without removing the ligands from the media. Results presented in figure 3A are striking, polymersome uptake is significantly inhibited in the presence of Fucoidan by FaDu cells (upper panel), and is almost abolished by NOF (lower panel), reaching fluorescent levels similar to untreated cells. Pre-incubation with polyinosinic acid did not affect polymersomes uptake by FaDu cells (Figure 3B-upper panel). However, only the highest concentration of polyinosinic acid (0.25 mg/ml) produced a slight, although significant, decrease in polymersome uptake ($p<0.05$) by NOF (Figure 3B-lower panel). These data suggest that type B scavenger receptors play a major role in polymersome uptake. So far three forms of type B scavenger receptors have been identified:

CD36, SR-BI and SR-BII, with the last two being splice variants of the same gene with each protein having the same extracellular loop but distinct cytoplasmic C-termini[38]. With the aim to differentiate which subtype of class B scavenger receptor is responsible for the binding of PMPC-PDPA polymersomes, we incubated FaDu and HDF with specific blocking antibodies against the extracellular loop of either CD36 or SR-BI/II and studied the effect of this on polymersome uptake. As shown in Figure 3C, blockade of SR-BI/II dramatically inhibited polymersome uptake in FaDu cells but failed to prevent internalisation by HDF. In contrast, blockade of CD36 alone did not inhibit polymersome internalisation in FaDu or HDFs. Interestingly, HDF continued to internalise polymersomes when one of the class B scavenger receptors was neutralised but uptake was significantly abolished when binding to both receptors was inhibited. This suggests that both SR-BI/II and CD36 work independently but simultaneously in PMPC-PDPA polymersome uptake. This data indicates that when one of the receptors is blocked the other can compensate for it or that the two receptors work synergistically. Even though at a first glance it seems that CD36 does not play a role in polymersome uptake in FaDu cells, it can be observed in Figure 3D that in order to produce the same degree of inhibition half of the concentration of neutralising IgG is needed when both SR-BI/II and CD36 are blocked simultaneously compared to when only one receptor is inhibited (i.e. 0.02 mg/mL of SR-BI/II and CD36 in combination generates approximately the same inhibition as 0.04 mg/mL of anti SR-BI/II alone). These data strongly indicate a role for class B scavenger receptors in mediating polymersome internalisation by HNSCC cells, in particular SR-BI. It is possible that the polymersome membrane structure is similar to that of a class B scavenger receptor ligands and this interaction drives endocytosis of polymersomes. Further detailed

experiments defining the interaction of polymersomes with class B scavenger receptors are currently underway in our laboratory in order to define this interaction at the molecular level.

Characterisation of chemotherapeutically loaded polymersomes. Next we examined the efficiency of PMPC-PDPA polymersomes to encapsulate hydrophobic paclitaxel and hydrophilic doxorubicin, alone and in combination. Paclitaxel was encapsulated into PMPC-PDPA polymersomes by adding the drug to the polymer mixture in the organic phase prior to rehydration. By contrast, doxorubicin was added during the rehydration stage of polymersome formation. In the case of dual loaded polymersomes, the paclitaxel was incorporated first followed by sequential loading of the doxorubicin during rehydration. In all instances non-encapsulated drug was removed from polymersome-encapsulated drug by gel permeation chromatography. High-performance liquid chromatography analysis revealed that the encapsulation efficiency for single and dual loaded drugs was between 37.1% ± 13.5% and 49.1% ± 4.4%, demonstrating high reproducibility between polymer batches (Table 1). The loading capacity of paclitaxel into polymersomes was much higher than reported for liposomal preparations and can be attributed to the thicker hydrophobic bilayer in polymersomes[39]. Other groups have demonstrated both singular and dual loading of polymersomes with paclitaxel and doxorubicin using different polymers and methodologies for drug incorporation[40,25,41]. Chen *et al*, (2009) developed pH-sensitive PEG–PTMBPEC degradable polymersomes and demonstrated the controlled release of dual loaded paclitaxel and doxorubicin in a pH-dependent manner. In their studies drug release was significantly faster at mildly acidic pH compared to physiological pH[41]. Ahmed *et al*, (2006) reported that biodegradable polymersomes dual loaded with paclitaxel

and doxorubicin was able to permeate and reduce the volume of xenograft MDA-MB231 breast tumours in an *in vivo* model [25].

Physiological analysis of the polymersomes by dynamic light scattering (DLS) and transmission electron microscopy (TEM), showed that like previous studies[42] the polymersomes were spherical and had a Gaussian distribution with an average size of 208 ± 27.7 nm, 193.6 ± 7.8 nm, 224.5 ± 43.5 nm for the paclitaxel, doxorubicin and dual loaded polymersomes respectively (Table 1). After storage at 4°C for 6 weeks the polymersomes remained spherical but their average size was slightly larger (but not significantly so; supplementary figure S2 and S3) when the same polymersomes were analysed by DLS and TEM. These data show that drug encapsulated polymersomes can be produced with highly reproducible size and stability that is not lost over a period of storage.

Cytotoxicity of paclitaxel and doxorubicin loaded polymersomes to HNSCC cells in 2D culture. The ability of the polymersomes to deliver active drug was assessed in 2D monolayers of the HNSCC cell line FaDu (Figure 4) as this cell line was found to internalise polymersomes most rapidly. The cell response to paclitaxel, doxorubicin and dual loaded polymersomes as well as to empty polymersomes was assessed at 24 and 48 hours with increasing concentrations of drug and polymer respectively. Empty polymersomes were well tolerated at all concentrations and time points tested, confirming their biocompatibility as previously shown with other cell types[20,27] (Figure 4). After 24 hours, both free and polymersome-encapsulated drugs, either on their own or as combination therapy, killed FaDu cells in a dose-dependent manner (Figure 4). At 24 hours both paclitaxel (Figure 4A) and doxorubicin (Figure 4C) loaded polymersomes showed significantly (p<0.05) more killing compared to free drug alone at the two lower

polymer concentrations (10 and 50 µg/ml). By contrast, at 24 hours, dual loaded polymersomes (Figure 4E) significantly reduced cell survival at all concentrations compared to the free drugs (p<0.05) and also when compared to polymersome-encapsulated paclitaxel or doxorubicin alone, showing that combined polymersome-delivered therapy is much better than single drug encapsulated therapy. The effect of combinational therapy, delivered via nanoparticles, has been extensively reviewed and current evidence shows that this combinational therapy is highly dependent on the molar ratios of drugs and the sequence in which they are delivered[43]. In support of this, we observed that the cytotoxicity of dual loaded polymersomes is greater than polymersomes loaded with a single drug. Further studies to investigate the effect of varying drug ratios and use of different dosing schedules are now required.

As anticipated, after 48 hours cell death was more pronounced than at 24 hours in all treated cells. However, no difference in cell survival was observed between FaDu cells treated with polymersome-encapsulated drugs and free drug except for the highest dose of dual loaded polymersomes, which significantly reduced cell viability (p<0.05) (Figure 4). Polymersome-delivered chemotherapy killed HNSCC cells more compared to free drug after 24 hours, suggesting that polymersome-mediated drug delivery could show a significant improvement in treatment response. However, this increased killing appears to be lost at 48 hours exposure and indicates that the benefit seen in polymersome-mediated therapy is due to the initial rapid uptake of the drug. This advantage may be magnified *in vivo* where tumours are only exposed to drugs delivered via the circulation for a short period of time, making quick cellular uptake crucial for a drug's success.

Cytotoxicity of single and combined drug-loaded polymersomes to FaDu monolayers after short exposure times. To determine if the rapid uptake kinetics of the polymersome-encapsulated drugs was important for the improved cancer cell cytotoxicity over free drug, FaDu monolayers were incubated with drug-loaded polymersomes or free drug alone or in combination for up to 60 minutes. The drugs were then removed and cell viability measured after 24 and 96-hour culture in drug-free medium. After 24 hours the cell viability was reduced in an exposure time-dependent manner for both encapsulated and free drug treated cells. In addition, there was a significant overall reduction in the cell viability with the paclitaxel and dual loaded (Figure 5A&E) polymersomes compared to their free drug equivalents at the 30 and 60 minute exposure times. Encapsulated doxorubicin displayed little cytotoxic advantage over free drug at these time points. Short exposure of polymersomes alone had no significant effect on cell survival after 24 or 96 hours (Supplementary Figure S4).

As expected the cytotoxic effect of all drugs was greatest after 96 hours culture post-exposure (Fig 5B, D and F). At this time point the killing achieved by encapsulated paclitaxel was nearly twice that achieved by free drug after only 10 minutes initial incubation (Figure 5B) and significantly more cancer cell killing was observed with encapsulated paclitaxel after 30 and 60 minutes compared to free paclitaxel alone. Interestingly, encapsulated doxorubicin showed equivalent or less cytotoxicity than the free drug alone after 96 hours, suggesting that free doxorubicin is able to penetrate into the cell without the requirement of polymersomes (Figure 5D). However, there is an increase in cell killing following short exposures for polymersome-encapsulated combinational chemotherapy compared to free combined drug treatment (Figure 5F). These data suggest that, after short exposure times, encapsulated paclitaxel is mainly responsible for cell cytotoxicity while encapsulated doxorubicin alone has little effect. However,

when these encapsulated drugs are combined enhanced killing is achieved. This may be because the cytotoxic action of paclitaxel is required for doxorubicin to exert its cytotoxic affects at short incubation times. It is possible that the action of paclitaxel on intracellular microtubule formation may disrupt the efflux of internalised doxorubicin thereby increasing its intracellular concentration and thus, cell cytotoxicity. Ahmed *et al* (2006) demonstrated that paclitaxel and doxorubicin loaded PEG-based polymersomes reduced the size of breast tumours grown subcutaneously in nude mice, demonstrating the clinical advantage of combination therapy[25].

Polymersome internalisation and cytotoxicity in a 3D model of HNSCC. MCTS are 3D cell culture models that possess a number of features similar to solid, expanding tumours *in vivo.* These features include a proliferative outer ring of cells, an inner hypoxic and necrotic core and a nutrient and pH gradient throughout the tissue which closely models naturally occurring tumours[44]. It is becoming widely accepted that testing drugs and delivery vehicles in MCTS is an essential step in drug development and improves the chances of selecting drugs which will be successful *in vivo*[45]. Here we used a FaDu MCTS model to study the diffusion of polymersomes into solid tumours and also the effects of drug-loaded polymersomes. Firstly, we investigated by both flow cytometry and fluorescence microscopy whether rhodamine-conjugated polymersomes were able to penetrate into MCTS. The internalisation kinetics of polymersomes into cells cultured as a MCTS was much slower compared to cells cultured as monolayers. This is because the polymersomes have to travel through layers of tumour cells to gain access to ones that are deeper in the tumour mass and this takes longer than gaining entry into cells cultured as monolayers. After 24 hours 20% of the cells within the MCTS contained polymersomes and this increased overtime and by five days over 80% of the cells within the MCTS contained

polymersomes (Figure 6A). Figure 6B shows representative cross sections of the MCTS after 0, 6, 24 and 120 hours. Polymersomes gradually penetrate into the MCTS from the surface and by five days are visible throughout the entire spheroid. These results are extremely promising as it is the central, hypoxic core of solid tumours that present the greatest challenge for treatment[46]. This is because drugs as well as oxygen can only diffuse approximately 200 μm into tissues and so the hypoxic centres of tumours are protected from the effects of chemotherapy. In fact, an increase in hypoxia in tumours is linked to poor prognosis in many cancers including HNSCC[46]. It is encouraging that these polymersomes, which are greater than 200 nm in diameter, were able to penetrate into the core of the MCTS as it has previously been found that nanoparticles greater than 100 nm diameter are impeded by the extracellular matrix and require enzymatic assistance to reach the core[45]. The most likely route by which the polymersomes reach the core of MCTS is by polymersome deformation. We have previously shown that the high level of entanglement in the hydrophobic membrane of PMPC-PDPA polymersomes enables polymersomes as large as 400 nm in diameter to deform sufficiently to cross a 50 nm pore membrane. These polymersomes retain structural integrity and are able to retain their encapsulated load even after deformation[47]. As polymersomes gain access to these central, hypoxic tumour areas they may rupture outside the cell because of the low pH of the tumour microenvironment at these sites. This in fact may be advantageous as hypoxic cells at these central tumour sites will be using anaerobic respiration and so will be unlikely to up-take polymersomes by endocytosis which is a highly energy-dependent process. Polymersomes and their load may also be delivered via the transcellular route via recurrent endocytosis and exocytosis; however this has yet to be investigated.

Drug-loaded polymersomes were then added to the MCTS and their effects on MCTS morphology and metabolic activity compared to empty polymersomes and free drug controls. Architecturally, after 24 hours the drug-encapsulated polymersome-treated MCTS retained structural integrity similar to that of the empty polymersome-treated controls, although the sizes of drug-treated MCTS were smaller than the controls (628 μm compared to 473 μm, 478 μm, 537 μm for paclitaxel, doxorubicin and dual loaded, respectively). However, after 96 hours exposure to polymersome-encapsulated chemotherapy and free drugs the MCTS architecture was completely disrupted compared to controls due to loss of cell viability (Figure 6C). Moreover, an MTT assay showed a trend towards better killing of MCTS with drug-loaded polymersomes compared to free drugs, however this did not reach statistical significance (Figure 6D). This demonstrates that after short exposure times the growth of the tumour is inhibited and with longer exposure the polymersomes and their encapsulated drugs are able to reach the central core, causing cytotoxicity throughout the MCTS. This is encouraging as the MCTS model provides a better representation of a naturally occurring tumour and demonstrates that these drug-loaded polymersomes are able to exert their cytotoxic effect to the central core of tumours.

In conclusion, we have shown rapid uptake of pH-sensitive PMPC-PDPA polymersomes into HNSCC cells. Polymersomes were preferentially taken-up by cancer cells and this is likely to be due to their higher expression of scavenger receptors. Most importantly, we report for the first time the high affinity binding of a fully synthetic polymer with these receptors. We have also demonstrated the ability to encapsulate paclitaxel and doxorubicin in combination into polymersomes and have shown that polymersome mediated drug delivery increases the cytotoxicity compared to free drugs. The potential of superficially targeting tumour cells by

conjugating tumour-specific ligands to the surface of polymersomes[48] may further decrease off-target cytotoxicity and reduce the levels of drugs needed to achieve systemic coverage.

Acknowledgments:

The authors would like to thank Dr Emma Hinsley and Sue Newton for technical assistance. This study was funded by a Yorkshire Cancer Research Project grant awarded to MT (PI), CM, GB and SA and an EPSRC studentship awarded to Vanessa Hearnden.

Supporting Information Available:

Figures S1-S4. This information is available free of charge via the Internet at http://pubs.acs.org/.

Drug(s)	Initial drug conc. (μg/ml)	Encapsulated drug conc. (μg/ml)	Encapsulation efficiency (%)	Average Size (nm)
Paclitaxel	250	112.3 ± 17.6	44.8 ± 8.6	208 ± 27.7
Doxorubicin	250	122.7 ± 9	49.1 ± 4.4	193.6 ± 7.8
Paclitaxcel + Doxorubicin	250 250	106.7 ± 20.8 92.3 ± 27.8	42.7 ± 10.2 37.1 ± 13.5	224.5 ± 43.5

Table 1. Encapsulation efficiency and size of drug-containing polymersomes used in this study. Data is compiled from three independent batches and is expressed as mean ± SD.

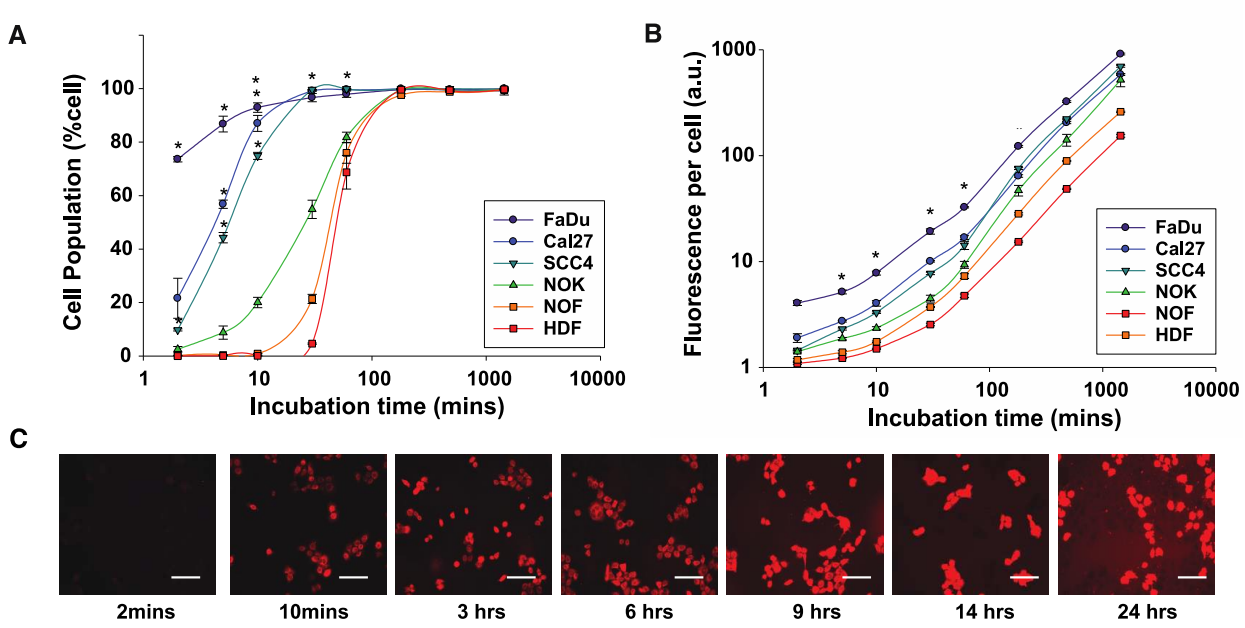

Figure 1. Polymersome internalisation kinetics. Internalisation studies of polymersomes into three HNSCC cell lines (Cal 27, FaDu and SCC4) and three primary cells types (NOK, NOF and HDF). Rhodamine-labelled PMPC-PDPA polymersomes (1 mg/ml) were added to cell monolayers and incubated at 37°C for increasing lengths of time. Cells were analysed using flow cytometry and the percentage of cells with fluorescence above control cells (A) and median fold increase in fluorescence of whole cell population calculated (B). Representative fluorescent microscopy images are shown for the polymersome uptake into FaDu cells (C). Scale = 100 µm. * denotes a statistically significant difference (One-way Independent ANOVA, $p<0.05$) of polymersome uptake into the different cancer cell lines compared to NOK.

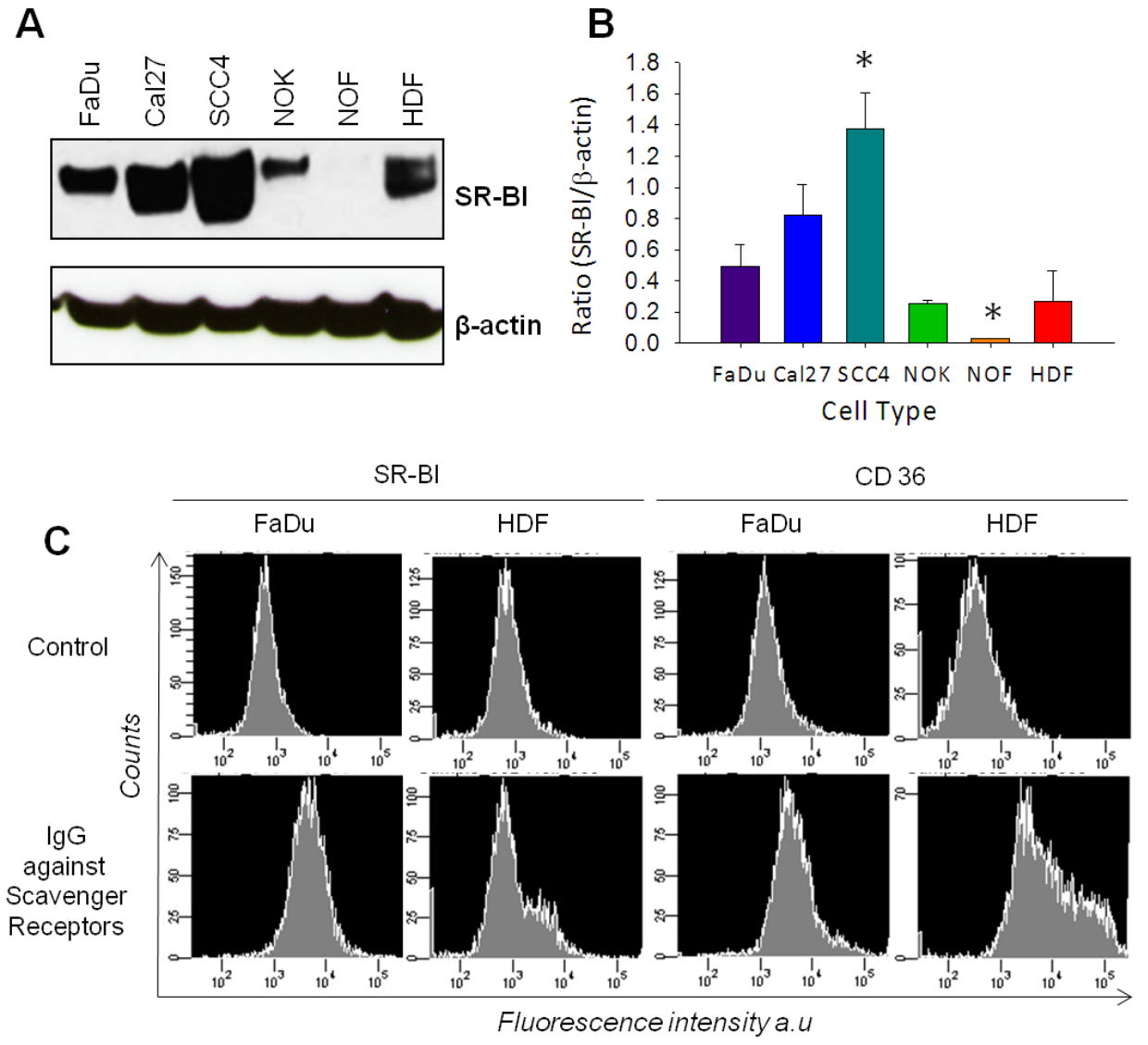
A
FaDu
Cal27
SCC4
NOK
NOF
HDF
SR-BI
β-actin
B
Ratio (SR-BI/β-actin)
1.8
1.6
1.4
1.2
1.0
0.8
0.6
0.4
0.2
0.0
*
*
FaDu Cal27 SCC4 NOK NOF HDF
Cell Type
C
SR-BI
CD 36
FaDu
HDF
FaDu
HDF
Control
IgG against Scavenger Receptors
Counts
Fluorescence intensity a.u
D
FaDu
HDF
***
**
100
50
0
% Fluorescent Cells
SR-BI
CD36

Figure 2. Evidence for functional scavenger receptors in FaDu and NOF cells. Cell lysates from HNSCC (FaDu, Cal27 and SCC4) and primary cells (HDF, NOF and NOK) were separated by SDS-PAGE and immunoblotting performed for SR-BI and β-actin (as a loading control). A representative blot is shown for SR-BI (A) and the intensity of the band determined by densitometry and normalised to β-actin levels in the same sample (B). For SR-BI n=3 * denotes a statistically significant difference from corresponding NOK expression (One way independent ANOVA, $p<0.05$).

(C) Expression of scavenger receptors assessed by flow cytometry in viable FaDu and HDF. Cells were first incubated with primary antibody targeting either SR-BI or CD36 scavenger receptors for 30 min at 4°C and then incubated with a fluorescently-labelled secondary antibody under the same conditions. (D) Percentage of fluorescent cells in each cell type normalised to control (wells treated just with secondary antibody). All experiments were performed in triplicate and each experiment was repeated independently three times. Data presented is representative of the three individual experiments. Error bars denote mean ± SEM. Statistical analysis: Student T-test where $*p<0.05$, $**p<0.01$, $***p<0.001$.

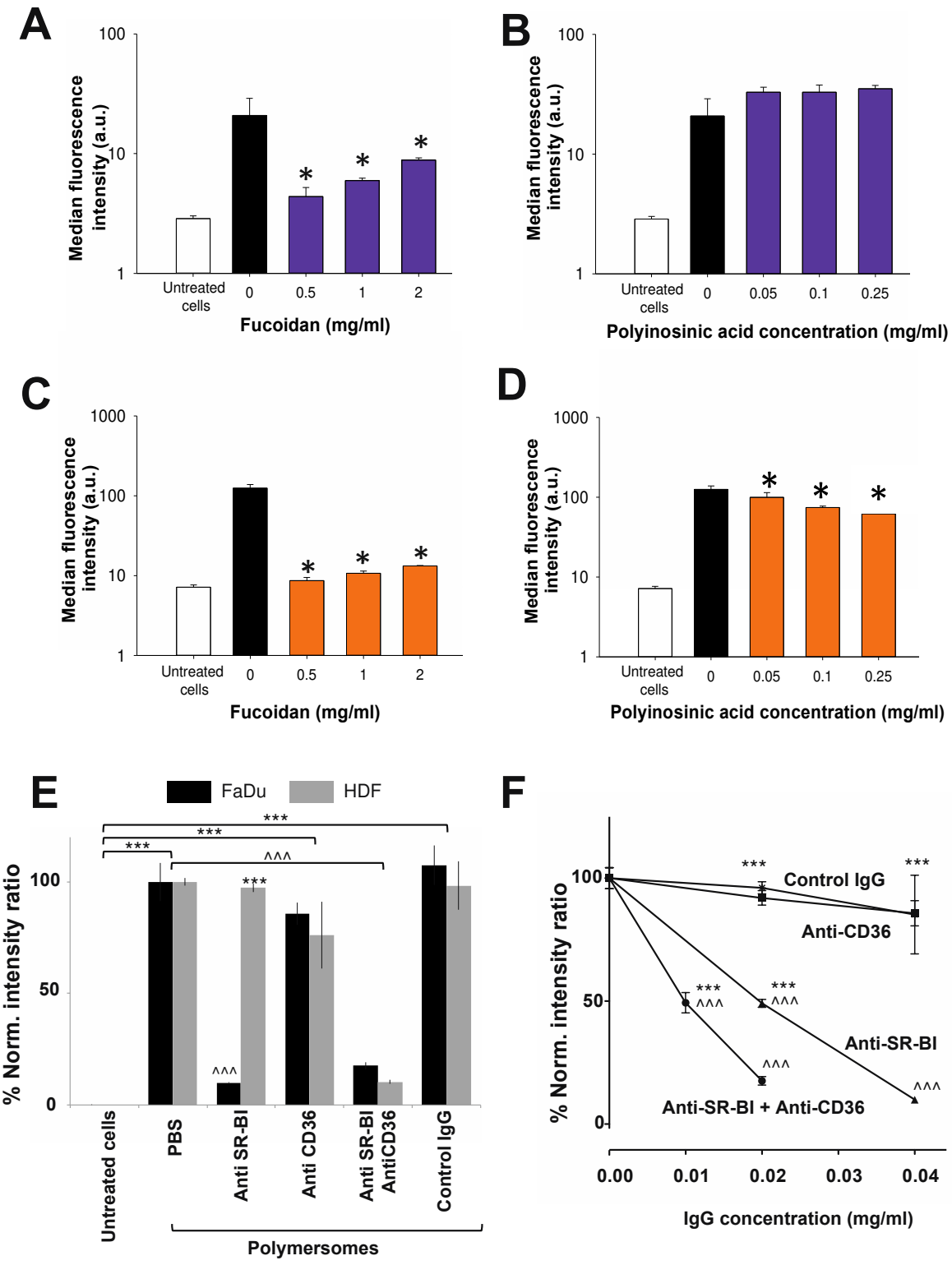
A
Median fluorescence intensity (a.u.)
100
10
1
Untreated cells
0
0.5
1
2
Fucoidan (mg/ml)
B
Median fluorescence intensity (a.u.)
100
10
1
Untreated cells
0
0.05
0.1
0.25
Polyinosinic acid concentration (mg/ml)
C
Median fluorescence intensity (a.u.)
1000
100
10
1
Untreated cells
0
0.5
1
2
Fucoidan (mg/ml)
D
Median fluorescence intensity (a.u.)
1000
100
10
1
Untreated cells
0
0.05
0.1
0.25
Polyinosinic acid concentration (mg/ml)
E
FaDu
HDF
% Norm. intensity ratio
100
50
0
Untreated cells
PBS
Anti SR-BI
Anti CD36
Anti SR-BI AntiCD36
Control IgG
Polymersomes
F
% Norm. intensity ratio
100
50
0
Control IgG
Anti-CD36
Anti-SR-BI
Anti-SR-BI + Anti-CD36
0.00
0.01
0.02
0.03
0.04
IgG concentration (mg/ml)

Figure 3. Effect of scavenger receptors inhibition in polymersome uptake. (A-B) FaDu and (C-D) NOF cells were pre-incubated for 1 h either with Fucoidan or polyinosinic acid. Rhodamine-labelled PMPC-PDPA polymersomes (1 mg/ml) were added afterwards to the wells and cells were incubated for another hour with polymersomes in the presence of the aforementioned ligands. Fluorescence intensities associated with the cells after the different treatments were measured by flow cytometry. (E) FaDu and HDF cells were pre-incubated for 1 h with specific antiserum against either SR-BI/II, CD36, a cocktail of both antibodies, or IgG as a control. Rhodamine-labelled PMPC-PDPA polymersomes (1 mg/ml) were added to the wells and cells were incubated for 1 h with polymersomes in the presence of the blocking antiserum. Fluorescence intensities associated with the cells after the different treatments were measured by flow cytometry. F) Titration of anti-scavenger receptor type B antibody concentrations in FaDu cells. Cells were treated following the same protocol as in C). Data are shown for n=3 and are representative of three independent experiments. Error bars denote ± SEM. Statistical analysis: * symbolises statistically significant difference (One-way Anova, * $p< 0.05$, ** $p<0.01$, *** $p<0.001$) between untreated cells (negative control) and the different treated groups. ^ symbolises statistically significant difference (One-way Anova, ^ ^ ^ $p<0.001$) between cells incubated just with polymersomes (positive control) and groups pre-incubated with scavenger receptor ligands/antibodies.

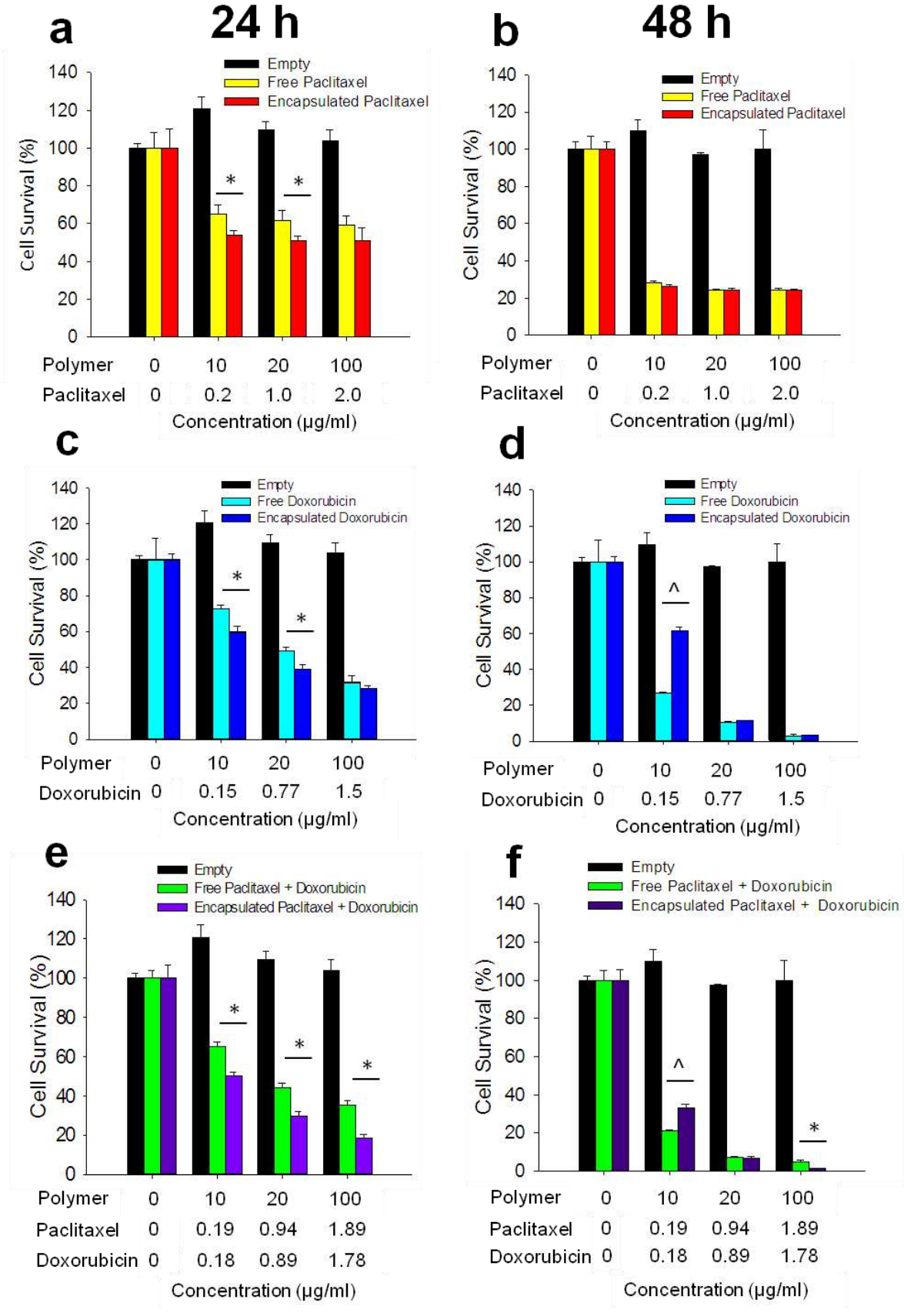
a
24 h
Empty
Free Paclitaxel
Encapsulated Paclitaxel
Cell Survival (%)
Polymer 0 10 20 100
Paclitaxel 0 0.2 1.0 2.0
Concentration (µg/ml)
b
48 h
Empty
Free Paclitaxel
Encapsulated Paclitaxel
Cell Survival (%)
Polymer 0 10 20 100
Paclitaxel 0 0.2 1.0 2.0
Concentration (µg/ml)
c
Empty
Free Doxorubicin
Encapsulated Doxorubicin
Cell Survival (%)
Polymer 0 10 20 100
Doxorubicin 0 0.15 0.77 1.5
Concentration (µg/ml)
d
Empty
Free Doxorubicin
Encapsulated Doxorubicin
Cell Survival (%)
Polymer 0 10 20 100
Doxorubicin 0 0.15 0.77 1.5
Concentration (µg/ml)
e
Empty
Free Paclitaxel + Doxorubicin
Encapsulated Paclitaxel + Doxorubicin
Cell Survival (%)
Polymer 0 10 20 100
Paclitaxel 0 0.19 0.94 1.89
Doxorubicin 0 0.18 0.89 1.78
Concentration (µg/ml)
f
Empty
Free Paclitaxel + Doxorubicin
Encapsulated Paclitaxel + Doxorubicin
Cell Survival (%)
Polymer 0 10 20 100
Paclitaxel 0 0.19 0.94 1.89
Doxorubicin 0 0.18 0.89 1.78
Concentration (µg/ml)

Figure 4. Encapsulated drugs vs free drug cytotoxicity after 24 and 48 hours exposure. Paclitaxel (A-B), doxorubicin (C-D) or dual loaded polymersomes (E-F) were incubated with FaDu monolayers for either 24 (left panel) or 48 h (right panel) and compared to free drug or empty polymersome equivalents. An MTT assay was used to determine the percentage cell survival and the data normalised to empty polymersomes control. All experiments were performed in triplicate and each experiment was repeated independently three times. Data presented is representative of the three individual experiments. * denotes a statistically significant difference from corresponding free drug equivalents (Student's *t*-test, $p < 0.05$) and ^ denotes a statistically significant difference from corresponding polymersome encapsulated drug (Student's *t*-test, $p < 0.05$). Error bars ± SD.

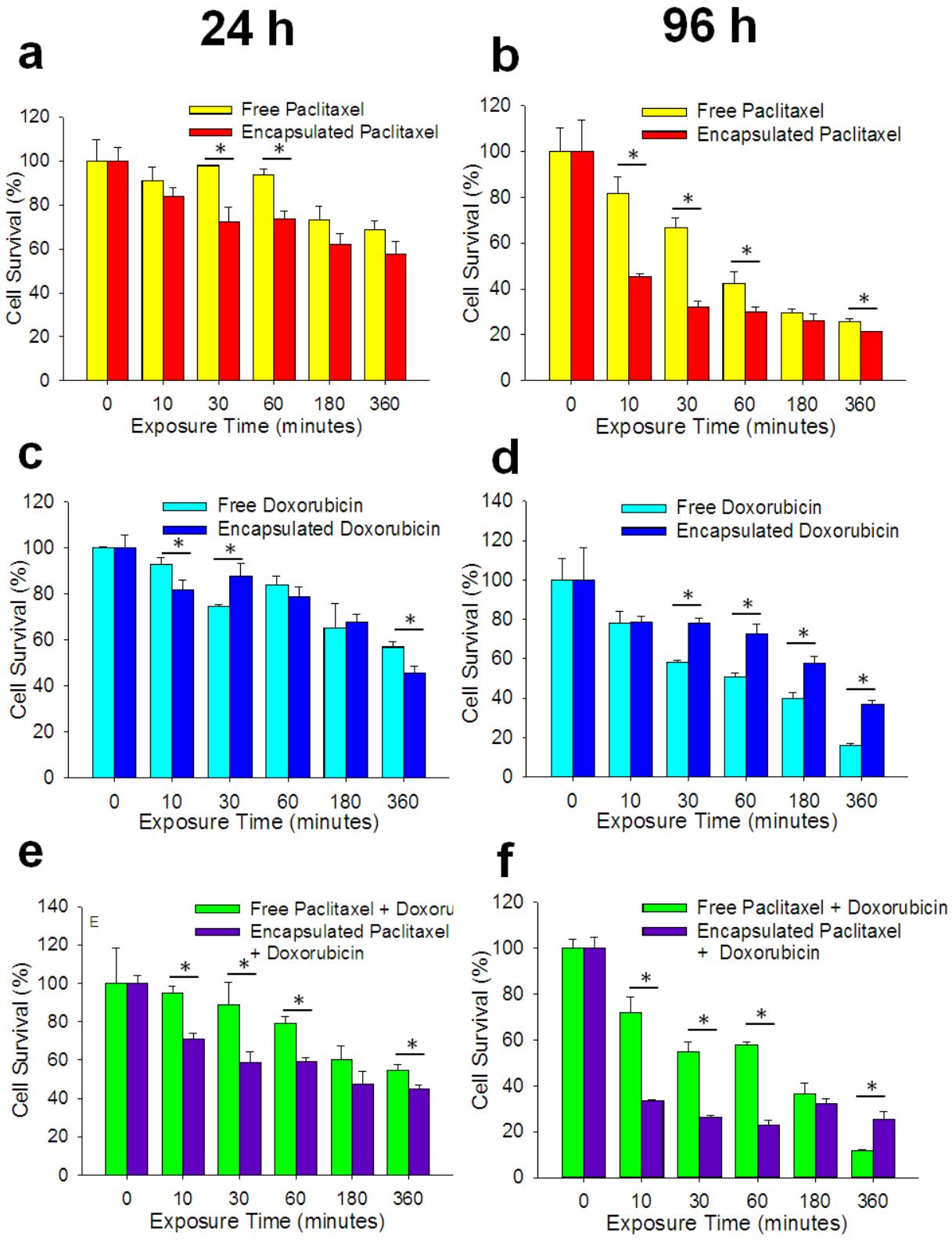
24 h
96 h
a
b
c
d
e
f
Free Paclitaxel
Encapsulated Paclitaxel
Free Doxorubicin
Encapsulated Doxorubicin
Free Paclitaxel + Doxoru
Encapsulated Paclitaxel
+ Doxorubicin
Free Paclitaxel + Doxorubicin
Cell Survival (%)
Exposure Time (minutes)
0
10
30
60
180
360
*

Figure 5. Encapsulated drugs vs free drug cytotoxicity after short exposure. Paclitaxel (A-B), doxorubicin (C-D) or dual loaded polymersomes (E-F) were incubated with FaDu monolayers for (10, 30, and 60 minutes) before additional culture for 24 (left panel) or 96 h (right panel) and compared to the same dose of free drug. An MTT assay was used to determine the percentage cell survival and the data normalised to empty polymersomes control. All experiments were performed in triplicate and each experiment was repeated independently three times. Data presented is representative of the three individual experiments. * denotes a statistically significant difference from the corresponding free drug equivalents (Student's *t*-test, $p < 0.05$). Error bars ± SD.

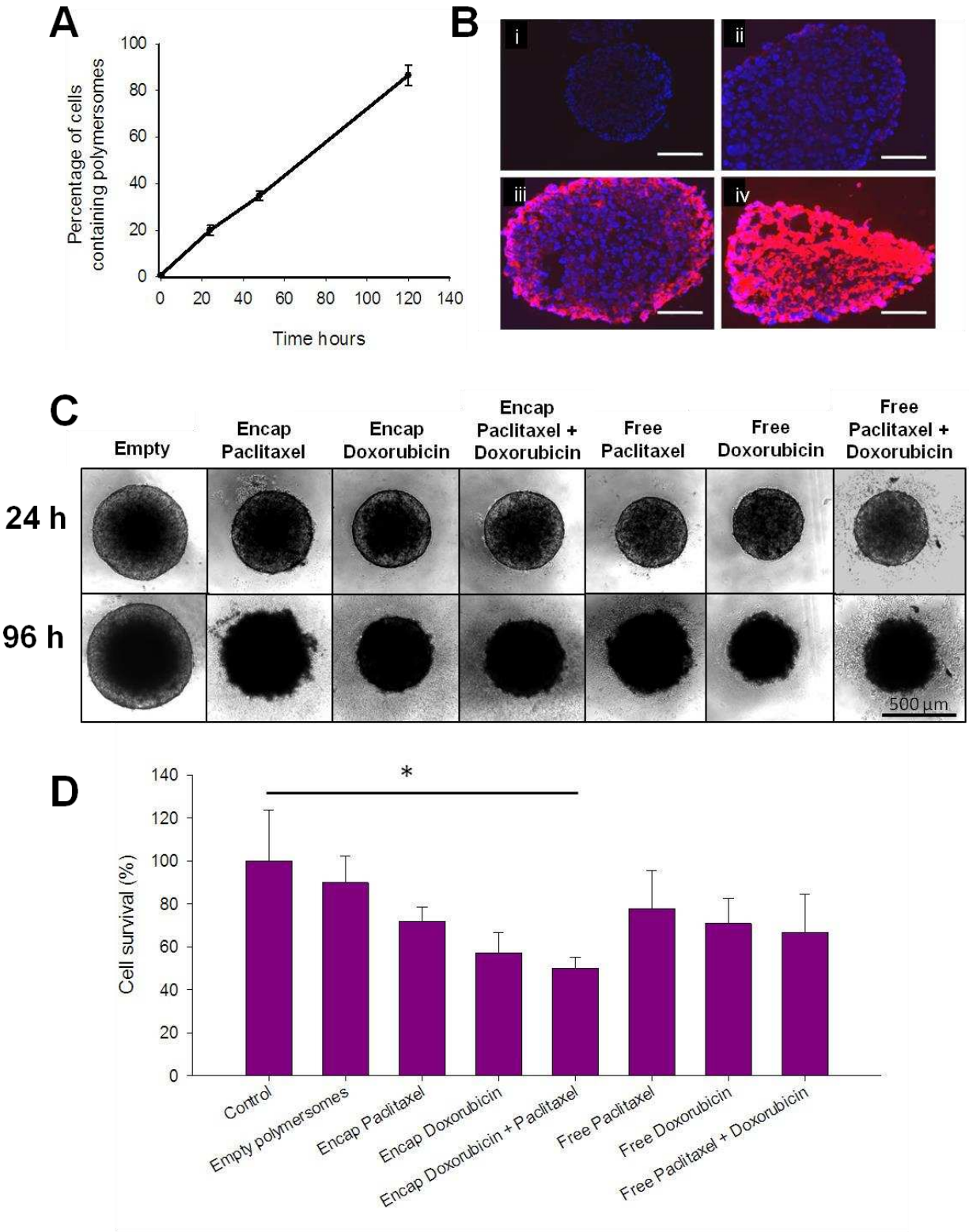
A
Percentage of cells containing polymersomes
100
80
60
40
20
0
0 20 40 60 80 100 120 140
Time hours
B
i
ii
iii
iv
C
Empty
Encap Paclitaxel
Encap Doxorubicin
Encap Paclitaxel + Doxorubicin
Free Paclitaxel
Free Doxorubicin
Free Paclitaxel + Doxorubicin
24 h
96 h
500 µm
D
*
Cell survival (%)
140
120
100
80
60
40
20
0
Control
Empty polymersomes
Encap Paclitaxel
Encap Doxorubicin
Encap Doxorubicin + Paclitaxel
Free Paclitaxel
Free Doxorubicin
Free Paclitaxel + Doxorubicin

Figure 6. Diffusion of polymersomes into an in vitro 3D tumour model. Internalisation studies of empty and drug loaded polymersomes into FaDu MCTS. Rhodamine-labelled polymersomes (1 mg/ml) were incubated with MCTS for increasing length of time (24, 48, 96 and 120 h). MCTS were disaggregated and individual cells analysed using flow cytometry and the percentage of cells with fluorescence above control cells calculated (A). Representative fluorescent microscopy images are shown for 0, 6, 24 and 120 h time points. Scale bar= 100 µm (B). Light microscopy images reveal that drug loaded polymersomes (1 µg/ml) are able to disrupt normal tumour architecture after 96 hours. Scale bar= 500 µm (C). MTT assay showing percentage cell survival after treatment with either free or polymersome encapsulated drug (D). * $p<0.05$ tested using ANOVA and Bonferroni test for multiple comparisons.

References

1. Volkova, M.; Russell, R., 3rd, Anthracycline cardiotoxicity: prevalence, pathogenesis and treatment. *Current cardiology reviews* **2011,** *7* (4), 214-20.
2. Singla, A. K.; Garg, A.; Aggarwal, D., Paclitaxel and its formulations. *International journal of pharmaceutics* **2002,** *235* (1-2), 179-92.
3. Weiszhar, Z.; Czucz, J.; Revesz, C.; Rosivall, L.; Szebeni, J.; Rozsnyay, Z., Complement activation by polyethoxylated pharmaceutical surfactants: Cremophor-EL, Tween-80 and Tween-20. *Eur J Pharm Sci* **2012,** *45* (4), 492-8.
4. Matsumura, Y.; Maeda, H., A new concept for macromolecular therapeutics in cancer chemotherapy: mechanism of tumoritropic accumulation of proteins and the antitumor agent smancs. *Cancer research* **1986,** *46* (12 Pt 1), 6387-92.
5. Barenholz, Y., Doxil(R)--the first FDA-approved nano-drug: lessons learned. *J Control Release* **2012,** *160* (2), 117-34.
6. von Gruenigen, V.; Frasure, H.; Fusco, N.; DeBernardo, R.; Eldermire, E.; Eaton, S.; Waggoner, S., A double-blind, randomized trial of pyridoxine versus placebo for the prevention of pegylated liposomal doxorubicin-related hand-foot syndrome in gynecologic oncology patients. *Cancer* **2010,** *116* (20), 4735-43.
7. Mross, K.; Niemann, B.; Massing, U.; Drevs, J.; Unger, C.; Bhamra, R.; Swenson, C. E., Pharmacokinetics of liposomal doxorubicin (TLC-D99; Myocet) in patients with solid tumors: an open-label, single-dose study. *Cancer Chemother Pharmacol* **2004,** *54* (6), 514-24.
8. Koudelka, S.; Turanek, J., Liposomal paclitaxel formulations. *Journal of Controlled Release* **2012,** *163* (3), 322-334.
9. Moghimi, S. M.; Peer, D.; Langer, R., Reshaping the future of nanopharmaceuticals: ad iudicium. *ACS nano* **2011,** *5* (11), 8454-8.
10. Schroeder, A.; Heller, D. A.; Winslow, M. M.; Dahlman, J. E.; Pratt, G. W.; Langer, R.; Jacks, T.; Anderson, D. G., Treating metastatic cancer with nanotechnology. *Nature reviews. Cancer* **2012,** *12* (1), 39-50.
11. Duncan, R., The dawning era of polymer therapeutics. *Nature reviews. Drug discovery* **2003,** *2* (5), 347-60.
12. Discher, D. E.; Eisenberg, A., Polymer vesicles. *Science* **2002,** *297* (5583), 967-73.
13. LoPresti, C.; Lomas, H.; Massignani, M.; Smart, T.; Battaglia, G., Polymersomes: nature inspired nanometer sized compartments. *Journal of Materials Chemistry* **2009,** *19* (22), 3576-3590.
14. Massignani, M.; Lomas, H.; Battaglia, G., Polymersomes: A Synthetic Biological Approach to Encapsulation and Delivery. In *Modern Techniques for Nano- and Microreactors/-reactions*, Caruso, F., Ed. Springer Berlin Heidelberg: 2010; Vol. 229, pp 115-154.
15. Lee, J. S.; Ankone, M.; Pieters, E.; Schiffelers, R. M.; Hennink, W. E.; Feijen, J., Circulation kinetics and biodistribution of dual-labeled polymersomes with modulated surface charge in tumor-bearing mice: comparison with stealth liposomes. *J Control Release* **2011,** *155* (2), 282-8.
16. Acton, S. L.; Scherer, P. E.; Lodish, H. F.; Krieger, M., Expression cloning of SR-BI, a CD36-related class B scavenger receptor. *The Journal of biological chemistry* **1994,** *269* (33), 21003-9.
17. Sankar, V.; Hearnden, V.; Hull, K.; Juras, D. V.; Greenberg, M. S.; Kerr, A. R.; Lockhart, P. B.; Patton, L. L.; Porter, S.; Thornhill, M., Local drug delivery for oral mucosal diseases: challenges and opportunities. *Oral Dis* **2011,** *17 Suppl 1*, 73-84.
18. Hearnden, V.; Lomas, H.; Macneil, S.; Thornhill, M.; Murdoch, C.; Lewis, A.; Madsen, J.; Blanazs, A.; Armes, S.; Battaglia, G., Diffusion studies of nanometer polymersomes across tissue engineered human oral mucosa. *Pharmaceutical research* **2009,** *26* (7), 1718-28.

19. Massignani, M.; LoPresti, C.; Blanazs, A.; Madsen, J.; Armes, S. P.; Lewis, A. L.; Battaglia, G., Controlling cellular uptake by surface chemistry, size, and surface topology at the nanoscale. *Small* **2009,** *5* (21), 2424-32.
20. Lomas, H.; Massignani, M.; Abdullah, K. A.; Canton, I.; Lo Presti, C.; MacNeil, S.; Du, J.; Blanazs, A.; Madsen, J.; Armes, S. P.; Lewis, A. L.; Battaglia, G., Non-cytotoxic polymer vesicles for rapid and efficient intracellular delivery. *Faraday Discuss* **2008,** *139*, 143-59; discussion 213-28, 419-20.
21. (a) Christian, D. A.; Cai, S.; Bowen, D. M.; Kim, Y.; Pajerowski, J. D.; Discher, D. E., Polymersome carriers: from self-assembly to siRNA and protein therapeutics. *Eur J Pharm Biopharm* **2009,** *71* (3), 463-74; (b) Canton, I.; Massignani, M.; Patikarnmonthon, N.; Chierico, L.; Robertson, J.; Renshaw, S. A.; Warren, N. J.; Madsen, J. P.; Armes, S. P.; Lewis, A. L.; Battaglia, G., Fully synthetic polymer vesicles for intracellular delivery of antibodies in live cells. *Faseb J* **2012,** *2012*, 2.
22. Massignani, M.; Canton, I.; Sun, T.; Hearnden, V.; Macneil, S.; Blanazs, A.; Armes, S. P.; Lewis, A.; Battaglia, G., Enhanced fluorescence imaging of live cells by effective cytosolic delivery of probes. *PloS one* **2010,** *5* (5), e10459.
23. Lomas, H.; Canton, I.; MacNeil, S.; Du, J.; Armes, S. P.; Ryan, A. J.; Lewis, A. L.; Battaglia, G., Biomimetic pH Sensitive Polymersomes for Efficient DNA Encapsulation and Delivery. *Advanced Materials* **2007,** *19* (23), 4238-4243.
24. Wang, L.; Chierico, L.; Little, D.; Patikarnmonthon, N.; Yang, Z.; Azzouz, M.; Madsen, J.; Armes, S. P.; Battaglia, G., Encapsulation of biomacromolecules within polymersomes by electroporation. *Angew Chem Int Ed Engl* **2012,** *51* (44), 11122-5.
25. Ahmed, F.; Pakunlu, R. I.; Brannan, A.; Bates, F.; Minko, T.; Discher, D. E., Biodegradable polymersomes loaded with both paclitaxel and doxorubicin permeate and shrink tumors, inducing apoptosis in proportion to accumulated drug. *J Control Release* **2006,** *116* (2), 150-8.
26. Price, K. A.; Cohen, E. E., Current treatment options for metastatic head and neck cancer. *Curr Treat Options Oncol* **2012,** *13* (1), 35-46.
27. Murdoch, C.; Reeves, K. J.; Hearnden, V.; Colley, H.; Massignani, M.; Canton, I.; Madsen, J.; Blanazs, A.; Armes, S. P.; Lewis, A. L.; Macneil, S.; Brown, N. J.; Thornhill, M. H.; Battaglia, G., Internalization and biodistribution of polymersomes into oral squamous cell carcinoma cells in vitro and in vivo. *Nanomedicine (Lond)* **2010,** *5* (7), 1025-36.
28. O'Neil, C. P.; Suzuki, T.; Demurtas, D.; Finka, A.; Hubbell, J. A., A novel method for the encapsulation of biomolecules into polymersomes via direct hydration. *Langmuir : the ACS journal of surfaces and colloids* **2009,** *25* (16), 9025-9.
29. Colley, H. E.; Hearnden, V.; Jones, A. V.; Weinreb, P. H.; Violette, S. M.; Macneil, S.; Thornhill, M. H.; Murdoch, C., Development of tissue-engineered models of oral dysplasia and early invasive oral squamous cell carcinoma. *Br J Cancer* **2011,** *105* (10), 1582-92.
30. Smith, L. E.; Hearnden, V.; Lu, Z.; Smallwood, R.; Hunter, K. D.; Matcher, S. J.; Thornhill, M. H.; Murdoch, C.; MacNeil, S., Evaluating the use of optical coherence tomography for the detection of epithelial cancers in vitro. *J Biomed Opt* **2011,** *16* (11), 116015.
31. Allen-Hoffmann, B. L.; Rheinwald, J. G., Polycyclic aromatic hydrocarbon mutagenesis of human epidermal keratinocytes in culture. *Proc Natl Acad Sci U S A* **1984,** *81* (24), 7802-6.
32. Araki, T.; Kono, Y.; Ogawara, K.; Watanabe, T.; Ono, T.; Kimura, T.; Higaki, K., Formulation and evaluation of paclitaxel-loaded polymeric nanoparticles composed of polyethylene glycol and polylactic acid block copolymer. *Biol Pharm Bull* **2012,** *35* (8), 1306-13.
33. (a) Mooberry, L. K.; Nair, M.; Paranjape, S.; McConathy, W. J.; Lacko, A. G., Receptor mediated uptake of paclitaxel from a synthetic high density lipoprotein nanocarrier. *Journal of drug targeting* **2010,** *18* (1), 53-8; (b) Saha, K.; Kim, S. T.; Yan, B.; Miranda, O. R.; Alfonso, F. S.; Shlosman, D.; Rotello, V. M., Surface Functionality of Nanoparticles Determines Cellular Uptake Mechanisms in Mammalian Cells. *Small* **2012,** *2012* (13), 201201129.

34. Hastie, C.; Saxton, M.; Akpan, A.; Cramer, R.; Masters, J. R.; Naaby-Hansen, S., Combined affinity labelling and mass spectrometry analysis of differential cell surface protein expression in normal and prostate cancer cells. *Oncogene* **2005,** *24* (38), 5905-13.
35. (a) Valacchi, G.; Sticozzi, C.; Lim, Y.; Pecorelli, A., Scavenger receptor class B type I: a multifunctional receptor. *Annals of the New York Academy of Sciences* **2011,** *1229*, E1-7; (b) Silverstein, R. L.; Febbraio, M., CD36, a scavenger receptor involved in immunity, metabolism, angiogenesis, and behavior. *Science signaling* **2009,** *2* (72), re3.
36. Patel, P. C.; Giljohann, D. A.; Daniel, W. L.; Zheng, D.; Prigodich, A. E.; Mirkin, C. A., Scavenger receptors mediate cellular uptake of polyvalent oligonucleotide-functionalized gold nanoparticles. *Bioconjugate chemistry* **2010,** *21* (12), 2250-6.
37. (a) Husemann, J.; Loike, J. D.; Kodama, T.; Silverstein, S. C., Scavenger receptor class B type I (SR-BI) mediates adhesion of neonatal murine microglia to fibrillar beta-amyloid. *Journal of neuroimmunology* **2001,** *114* (1-2), 142-50; (b) Haisma, H. J.; Kamps, J. A.; Kamps, G. K.; Plantinga, J. A.; Rots, M. G.; Bellu, A. R., Polyinosinic acid enhances delivery of adenovirus vectors in vivo by preventing sequestration in liver macrophages. *The Journal of general virology* **2008,** *89* (Pt 5), 1097-105.
38. Webb, N. R.; Connell, P. M.; Graf, G. A.; Smart, E. J.; de Villiers, W. J.; de Beer, F. C.; van der Westhuyzen, D. R., SR-BII, an isoform of the scavenger receptor BI containing an alternate cytoplasmic tail, mediates lipid transfer between high density lipoprotein and cells. *The Journal of biological chemistry* **1998,** *273* (24), 15241-8.
39. Crosasso, P.; Ceruti, M.; Brusa, P.; Arpicco, S.; Dosio, F.; Cattel, L., Preparation, characterization and properties of sterically stabilized paclitaxel-containing liposomes. *J Control Release* **2000,** *63* (1-2), 19-30.
40. Li, S.; Byrne, B.; Welsh, J.; Palmer, A. F., Self-assembled poly(butadiene)-b-poly(ethylene oxide) polymersomes as paclitaxel carriers. *Biotechnol Prog* **2007,** *23* (1), 278-85.
41. Chen, W.; Meng, F.; Cheng, R.; Zhong, Z., pH-Sensitive degradable polymersomes for triggered release of anticancer drugs: a comparative study with micelles. *J Control Release* **2010,** *142* (1), 40-6.
42. Blanazs, A.; Armes, S. P.; Ryan, A. J., Self-Assembled Block Copolymer Aggregates: From Micelles to Vesicles and their Biological Applications. *Macromolecular Rapid Communications* **2009,** *30* (4-5), 267-277.
43. Hu, C. M.; Aryal, S.; Zhang, L., Nanoparticle-assisted combination therapies for effective cancer treatment. *Ther Deliv* **2010,** *1* (2), 323-34.
44. Hirschhaeuser, F.; Menne, H.; Dittfeld, C.; West, J.; Mueller-Klieser, W.; Kunz-Schughart, L. A., Multicellular tumor spheroids: an underestimated tool is catching up again. *J Biotechnol* **2010,** *148* (1), 3-15.
45. Mehta, G.; Hsiao, A. Y.; Ingram, M.; Luker, G. D.; Takayama, S., Opportunities and challenges for use of tumor spheroids as models to test drug delivery and efficacy. *J Control Release* **2012,** *164* (2), 192-204.
46. Eckert, A. W.; Kappler, M.; Schubert, J.; Taubert, H., Correlation of expression of hypoxia-related proteins with prognosis in oral squamous cell carcinoma patients. *Oral and maxillofacial surgery* **2012,** *16* (2), 189-96.
47. Pegoraro, C.; MacNeil, S.; Battaglia, G., Transdermal drug delivery: from micro to nano. *Nanoscale* **2012,** *4* (6), 1881-94.
48. Kamphuis, M. M.; Johnston, A. P.; Such, G. K.; Dam, H. H.; Evans, R. A.; Scott, A. M.; Nice, E. C.; Heath, J. K.; Caruso, F., Targeting of cancer cells using click-functionalized polymer capsules. *J Am Chem Soc* **2010,** *132* (45), 15881-3.